

## ORIGINAL ARTICLE

# *LncRNA-H19* gene plays a significant role in regulating glioma cell function

Ping Liu | Xinqiong Huang | Haijun Wu | Guoling Yin | Liangfang Shen 

Department of Oncology, Heping Hospital Affiliated to Changzhi Medical College, Changzhi, China

**Correspondence**

Liangfang Shen, Department of Oncology, Heping Hospital Affiliated to Changzhi Medical College, Changzhi, China.

Email: fgbhwh@126.com

**Funding information**

None declared.

**Abstract**

**Background:** Glioma is an aggressive adult primary cancer, and is characterized by low cure rate, poor prognosis, and high recurrence. The present study aimed to investigate the effect of *lncRNA-H19* gene silencing on glioma cell function.

**Methods:** *lncRNA-H19* interference vector (LV3-si-H19) and negative control vector (LV3-NC) were stably transfected into U251 and U87-MG cells, respectively. Quantitative real-time PCR (qRT-PCR) was performed to investigate the expression of *lncRNA-H19*. Cell proliferation capacity was tested by adopting cell counting kit (CCK8), and propidium iodide (PI) was used for cell cycle analysis. Meanwhile, flow cytometry (FCM) method was used to investigate cell apoptosis, cell migration capacity was detected via wound healing and transwell experiments, and sphere-forming ability was examined in serum-free suspension culture. Additionally, glioma animal models were conducted through injecting U251 cells to estimate the effects of *lncRNA-H19* on glioma growth in vivo.

**Results:** Knocking down *lncRNA-H19* gene could effectively suppress the proliferation of U251 and U87-MG cells. The knockdown of *lncRNA-H19* remarkably inhibited the migration and blocked cycle progressions of U251 and U87-MG cells, yet, no obvious changes were observed in cell apoptosis. Besides, inhibiting *lncRNA-H19* expression could attenuate sphere-forming function of U251 and U87-MG cells. Additionally, tumor volume and weight were significantly reduced in rats injected with U251 LV-si-H19 cell line compared to untransfected and negative controls, when survival time was obviously prolonged in U251 LV-si-H19 injection groups.

**Conclusion:** *LncRNA-H19* gene plays a carcinogenic role in glioma progression via enhancing aggressive behavior of glioma cells.

**KEYWORDS**

animal model, biological behavior, Glioma cell, *LncRNA-H19* interference

## 1 | INTRODUCTION

Glioma is the most common type of primary intracranial tumors and is highly lethal due to its pathogenetic location, high

invasiveness, and poor prognosis (Gu et al., 2015). According to WHO classification, glioma can be divided into I, II, III, and IV grade levels, and malignancy degree increases with grade. Glioblastoma, classified as Class IV according to its biological

This is an open access article under the terms of the Creative Commons Attribution-NonCommercial License, which permits use, distribution and reproduction in any medium, provided the original work is properly cited and is not used for commercial purposes.

© 2021 The Authors. *Molecular Genetics & Genomic Medicine* published by Wiley Periodicals LLC.

behavior, represents the highest degree of malignancy, and the average one-year survival rate of its patients is only 46% (Allen, Huang, & Clarke, 2014). Currently, the most commonly applied method to treat gliomas is surgery, with adjuvant therapies like radiotherapy, chemotherapy, medicine, etc. Nevertheless, overall treatment effect is still not ideal, especially for those diagnosed with high-grade gliomas. A large number of studies have shown that among patients with glioma, even after standard combination therapy, the five-year survival rate is still poor. Therefore, it is urgent to identify sensitive biomarkers to treat glioma.

Recent studies have indicated that long noncoding RNAs (lncRNA) have important biological functions via regulating several important processes (Rossi & Antonangeli, 2014). Previous studies have shown that many lncRNAs exhibit cell-specific expressions and subcellular localization, and that their alterations may lead to various human diseases, such as prostate cancer, colon cancer, breast cancer, bladder cancer, liver cancer, brain tumor, etc. (Chen, Yao, Wang, & Liu, 2017; Gloss & Dinger, 2016; J. Li, Xue, et al., 2017; Prensner et al., 2013; Tracy et al., 2018; Wu et al., 2017; Zhang, Su, Lu, & Wang, 2013). *lncRNA-H19* (OMIM accession number: 103280; HGNC: 4713) is one of common lncRNAs, and has been observed in endoderm and mesoderm-derived tissues (Necsulea et al., 2014). It seats in conservative gene cluster, locating on human 11p15.5. (Monnier et al., 2013). *lncRNA-H19* is a maturely imprinted gene with a full-length of 2.5 kb, including five exons and four introns (Li, Yin, et al., 2017). *lncRNA-H19* plays an important role in maintaining normal physiological conditions, and its abnormal expression may result in pathological situations. Previous studies have reported that *lncRNA-H19* was related to various cancers including colorectal cancer (Yang, Ning, & Jin, 2017), bladder cancer (Hua et al., 2016), gastric cancer (Zhuang, Gao, Xu, Wang, & Shu, 2014), and a variety of tumors in central nervous system (Shi et al., 2014). However, biological function of *lncRNA-H19* in glioma biology and underlying mechanisms remain unclear.

In the present study, we aimed to explore biological function of *lncRNA-H19* in glioma. The present study might provide a new target for the management of glioma.

## 2 | MATERIALS AND METHODS

### 2.1 | Ethical compliance

This study was approved by the Ethics Committee of Heping Hospital Affiliated to Changzhi Medical College.

#### 2.1.1 | Cell lines and cultures

The following procedures were carried out in accordance with approved guidelines. All authors reviewed the results and approved the final version of the manuscript.

All experimental protocols were approved by Heping Hospital Affiliated to Changzhi Medical College. Glioma Cell U251 and U87-MG were purchased from Beijing Union Medical College Hospital. The cells were cultured in mixed medium DMEM containing 10% of fetal bovine serum (Invitrogen, Carlsbad, CA) at 37°C with 5% of CO<sub>2</sub>.

#### 2.1.2 | Construction of recombinant lentivirus

Small interfering RNA (siRNA) sequence targeting *lncRNA-H19* (NCBI reference sequence: NR\_002196.2) was 5'-GACGTGA CAAGCAGGACAT-3'. A scramble fragment 5'-GCAGATAGGTAGGCGTTAT-3' was used as negative control that had no significant homology to any human gene sequences. Stem-loop oligonucleotides (TTCAAGAGA) were synthesized and cloned into lentivirus-based vector LV3, and resulting plasmids were named as LV3-si-H19 and LV3-NC, respectively. Lentivirus packaging system including recombinant LV3-si-H19 plasmid or LV3-NC together with two packaging plasmids (psPAX2 and pMD2.G) was co-transfected into cells using Lipofectamine 2000 (Invitrogen). Then, lentiviral particles were harvested from the media 48 hr after transfection, from centrifuged supernatant (4000 g, 10 minutes, 4°C), and lentiviral particles were purified with 0.45 mm cellulose acetate filters. The titer of concentrated lentivirus was determined via dilution, adopting fluorescent microscopy.

#### 2.1.3 | Lentivirus infection

Cells were cultured in growth medium to 30% confluence at the time of transduction ( $2 \times 10^5$  cell/ml cells in 6-well plates), and then, transfected with LV3-si-H19 and LV3-NC at multiplicity of infection (MOI) of 1. Cells were harvested 72 hr after transduction and analyzed with FACS to sort and collect green fluorescent protein (GFP)-positive ones, which could be distinguished easily from untransfected ones by green fluorescent under fluorescence microscope.

#### 2.1.4 | Quantitative real-time PCR (qRT-PCR) analysis

Total RNA was isolated from cells with TRIzol reagent (Invitrogen) according to the manufacturer's instructions. Those total RNA samples with an OD A260/A280 ratio close to 2.0, which indicated that RNA was pure, were reversely transcribed into cDNA. Real-time PCR reactions using SYBR green (Invitrogen) were run on Applied Biosystems 7500 Real-Time PCR system (Applied Biosystems). Real-time PCR primers for *lncRNA-H19*

and beta-actin were designed and synthesized by Dingguo Changsheng Biotech. Primer sequences were as follows: *lncRNA-H19* forward 5'-CGGTCACCTTTGGTTA-3' and reverse 5'-GGAGGGTGTCTGCTTC-3', *β-actin* forward 5'-ATCATGTTTGAGA CCTTCAACA-3' and reverse 5'-CATCTCTTGCTC GAAGTCCA-3'.

### 2.1.5 | Cell proliferation analysis

Cell growth curves were obtained by measuring cell viability with Cell Counting Kit-8 (CCK-8, Dojindo, Japan) according to the manufacturer's instruction. After transduction for 72 hr, the cells in test groups were plated at a final concentration of 3,000 cells/well into 96-well culture plates for 5 days in a 37°C, 5% of CO<sub>2</sub> incubator. Then, the number of viable cells was measured on the first, second, third, fourth, and fifth days. At each time point, CCK8 (5 mg/ml) was added into each well and incubated at 37°C for 2 hr. Absorbance was measured at 450 nm using Microplate reader. Each group was measured in triplicate.

### 2.1.6 | Cell cycle analysis

The cells in test groups were seeded into 6-well culture plates ( $5 \times 10^5$ ) and harvested at 72 hr through centrifugation at 1200 rpm for 5 min. After washing twice with precooled DPBS, the cells were fixed in 70% of alcohol overnight at 4°C, and then, pelleted via centrifugation to remove stationary liquid. After that, the cells were washed twice using DPBS, and 100 μL of RNaseA (1 mg/ml) was added into each tube before additional incubation of 30 min at 37°C. At the end, propidium iodide (PI, Sigma) was added into each well, and incubated in dark at room temperature. Cell cycle distribution was analyzed using flow cytometer (FACSCalibur, BD).

### 2.1.7 | Apoptosis assay

Seventy-two hours after transfection, apoptotic U87-MG and U251 cells were labeled with annexin V-phycoerythrin (PE), mixed gently and incubated at 2–8°C for 15 min in dark. Then, 5 μl Annexin V-PE/7-AAD was added to each sample and incubated at 2–8°C for 5 min in dark. Then, fluorescence-activated apoptotic cells were categorized employing flow cytometer (BD FACSVantage™ SE, BD Biosciences Co., Franklin Lakes).

### 2.1.8 | Wound healing and cell transwell migration assays

Wound healing assay: Cells ( $5 \times 10^4$ ) were seeded on a 6-well plate and cultured for 72 hr. When cultured cells

covered the bottom of the plate, a scratch was made on cell monolayer with a 200 μL pipette tip. U251 was monitored with a microscope every 24 hr. U87-MG was monitored with a microscope every 6 hr. Cell migration was determined via the rate of cells filling the scratched area. Normalized wound area was calculated in the software PS.

Transwell assay: After incubated for 72 hr,  $5 \times 10^4$  cells were plated in 6-well transwell chamber in 3 ml complete medium. After 48 hr, the cells were washed twice with 1× PBS, and then, membranes were removed gently with a razor blade and rinsed. The cells that migrated through the membrane and attached to the bottom of the membrane were fixed and stained with hematoxylin. After washed for 2 min with water, new water was used to soak the membrane for 10 min. Mounted with neutral gum, under microscopy, cells in six randomly selected visual fields were counted. Tests were repeated via three independent experiments.

### 2.1.9 | Tumor sphere formation assay

Cells ( $3 \times 10^2$  cells / well) were seeded in ultralow adhesion 96-well, 3–6 wells each group. The cells were continuously incubated in incubator. To prevent cell adhesion, the 96-well was shaken twice a day, add medium was added to each well every 2–3 days. Cell balls were observed under light microscope. Cell spheres were photographed and those greater than 50 μm were counted.

### 2.1.10 | Animal model

Animal breeding and procedures were conducted in line with the Animal Care and Use Committee guidelines of our hospital. A total of 30 male rats were used to conduct in vivo experiments. The rats were divided into three groups, with 10 in each group.  $5 \times 10^5$  U251 cells (in 5 μL PBS) which were infected by LV3-si-H19 were inoculated into the right stratum (lateral: 2 mm; anterior to the bregma: 0.5 mm; depth: 3 mm) of the animals via a small animal stereotactic frame (RWD Life Science, Shenzhen, China). LV3-NC-infected U251 served as negative control, while U251 cells without infection were employed as untransfected controls.

### 2.1.11 | Tumor growth evaluation

After injection, tumor growth in animal model was observed using bioluminescence imaging technique and recorded every 5 days. Based on tumor size, tumor volume was calculated according to the following formula: tumor volume =  $a \times b^2 \times 0.5$ , a: the lengthy diameter; b: the short diameter. Sixty-day growth curve for tumor was plotted to

estimate the effects of *lncRNA-H19* expression on glioma growth.

Sixty days after tumor implantation, five rats in each group were sacrificed to isolate tumor specimens, and tumor inhibition rate was calculated. Tumor inhibition rate = [(the average tumor weight of control group - the mean weight of LV3-si-H19 group)/the average weight of control group] × 100%. Additionally, the expression level of *lncRNA-H19* in tumor specimens was also estimated using qRT-PCR.

### 2.1.12 | Survival estimation based on rat model

The rest five rats in each group were used for survival analysis. Rats in transfected group and control group faced similar conditions, and the survival time of each group was recorded to estimate the effects of *H19* expression on the survival of glioma.

### 2.1.13 | Statistical analysis

All data were expressed as mean ± standard error of the mean (SEM). Differences between two groups were compared using student's *t* test, and those among three groups were analyzed with ANOVA. Statistical analysis was performed using SPSS version 13.0 (SPSS Inc.). Results were considered statistically significant when  $p < 0.05$ .

## 3 | RESULTS

### 3.1 | Lentivirus-mediated siRNA inhibited the expression of *lncRNA-H19* in U251 and U87-MG cells

U251 and U87-MG cell lines were transfected with LV3-si-H19 and LV3-NC, with the highest transfection efficiency at 100%, which was determined via detecting the expression of green fluorescent protein (GFP) 72 hr after infection (Figure 1a). QRT-PCR analysis showed that *lncRNA-H19* expression level was significantly lower in LV3-si-H19 group than in LV3-NC group and untransfected group (Figure 1b,c).

### 3.2 | *lncRNA-H19* knockdown inhibited cell proliferation

The proliferation of U251 and U87-MG cells transfected by LV3-si-H19 was detected. LV3-NC group and untransfected group were used as controls, and experiment

was repeated five times. OD value was recorded once a day for 5 days adopting microplate reader, and data were presented in Table 1. For U251 cells, OD values were roughly same to those for untransfected group, negative control group and LV3-si-H19 interference group on the first and second days. OD values were increased, following cultured for 3 d, 4 d, and 5 d, along with number increased of the cultured cells, OD value of each group was also increased, and LV3-si-H19 group's OD values were significantly lower than those for the untransfected group and the LV3-NC group at the same time. For U87-MG cells, OD values were roughly same to those for the three group on the first day, without significant difference. After cultured for 2 d, 3 d, 4 d, and 5 d, OD value of each group was increased, and LV3-si-H19 group's OD values were significantly lower than those for the untransfected group and the LV3-NC group. *lncRNA-H19* silencing inhibited U251 and U87-MG cell proliferation in a time-dependent manner, as shown in Table 1 and Figure 2.

### 3.3 | *lncRNA-H19* knockdown induced cell cycle arrest

Flow cytometric analysis showed that the proportion of cells in G2/M phase was markedly increased in LV3-si-H19 group compared with LV3-NC group and untransfected group, but the proportion of cells in G0/G1 and S phases was markedly decreased in LV3-si-H19 group compared with LV3-NC group and untransfected group. The result indicated that *lncRNA-H19* knockdown could significantly inhibit cell cycle progression of U251 and U87-MG cells and arrest cell cycle in G2/M phase (Figure 3).

### 3.4 | *lncRNA-H19* knockdown affected cell apoptosis

Apoptosis was assessed via flow cytometry, and the results indicated that knocking down *H19* expression had no effect on apoptosis rate of glioma cells, compared with LV3-NC group and untransfected group (Figure 4).

### 3.5 | *lncRNA-H19* knockdown decreased the migration of glioma cells

Wound healing assays and Transwell assays were used to explore the effect of *lncRNA-H19* interference on the migration of glioma cells. The results of wound healing assay displayed that reduced *lncRNA-H19* expression blocked cell migration of U251 (Figure 5a,b) and U87-MG (Figure 5c,d). For U251, *lncRNA-H19* knockdown had no significant effect on cell

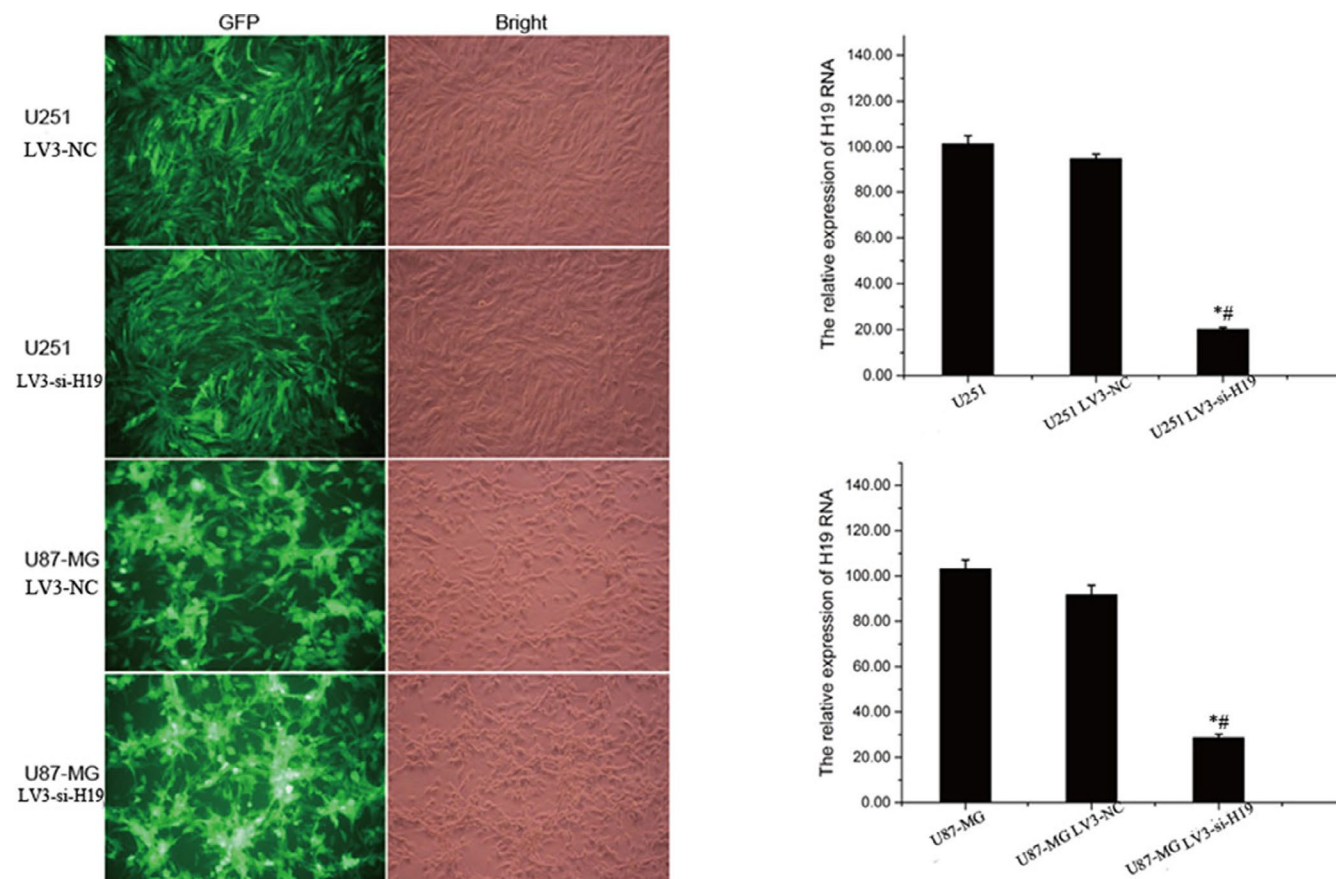


**FIGURE 1** Knockdown *lncRNA-H19* in glioma cells by lentivirus-mediated shRNA. (a) Detection of lentiviral infection efficiency, ( $\times 100$ ). The U251 and U87-MG cells were infected with LV3-si-H19 and LV3-NC, and GFP (right) or phase contrast (left) images were obtained 72 hr after infection. (b-c) Analyses of *lncRNA-H19* RNA expression in U251 and U87-MG cells by quantitative real-time. \* $p < 0.01$ , versus untransfected control group; # $p < 0.01$ , versus NC group. The NCBI reference sequence for *lncRNA-H19* was NR\_002196.2.

**TABLE 1** The effect of *lncRNA-H19*<sup>a</sup> knockdown on cell proliferation of U251 and U87-MG.

Samples	OD value				
	1 d	2 d	3 d	4 d	5 d
U251	0.56 $\pm$ 0.05	0.71 $\pm$ 0.01	0.94 $\pm$ 0.03	1.28 $\pm$ 0.05	1.95 $\pm$ 0.08
U251 NC	0.55 $\pm$ 0.05	0.69 $\pm$ 0.011	0.89 $\pm$ 0.05	1.13 $\pm$ 0.06	1.75 $\pm$ 0.02
U251Si-H19	0.50 $\pm$ 0.04 <sup>b</sup>	0.63 $\pm$ 0.019 <sup>b,c</sup>	0.66 $\pm$ 0.034 <sup>b,c</sup>	0.71 $\pm$ 0.03 <sup>b,c</sup>	0.90 $\pm$ 0.08 <sup>b,c</sup>
U87-MG	0.56 $\pm$ 0.04	0.64 $\pm$ 0.053	0.87 $\pm$ 0.01	1.11 $\pm$ 0.04	1.35 $\pm$ 0.06
U87-MG NC	0.51 $\pm$ 0.06	0.62 $\pm$ 0.011	0.87 $\pm$ 0.01	1.08 $\pm$ 0.07	1.32 $\pm$ 0.05
U87-MG Si-H19	0.48 $\pm$ 0.04 <sup>b</sup>	0.51 $\pm$ 0.04 <sup>c,d</sup>	0.55 $\pm$ 0.01 <sup>b,c</sup>	0.71 $\pm$ 0.03 <sup>b,c</sup>	0.83 $\pm$ 0.02 <sup>b,c</sup>

<sup>a</sup>NCBI reference sequence: NR\_002196.2.

<sup>b</sup> $p < 0.01$ , versus untransfected group.

<sup>c</sup> $p < 0.01$ , versus negative control group.

<sup>d</sup> $p < 0.05$ , versus untransfected group.

migration at 24 hr, but at 48 hr, inhibiting *lncRNA-H19* expression could significantly affect the migration of glioma cells compared to control groups. For U87-MG cells, *lncRNA-H19* knockdown showed no significant effect on cell migration at 6 hr, compared with control groups. Significant inhibitory effect emerged in LV3-si-H19-transfected group compared with

the untransfected group and the LV3-NC group at 12 hr hour. But after 24 hr, the three groups were all healed. We further investigated cell migration using transwell assay, and the result showed that *lncRNA-H19* knockdown could inhibit U251 cell and U87-MG cell migration (Figure 5e,f), and that inhibition rate was up to 39.17% and 32.14%, respectively.

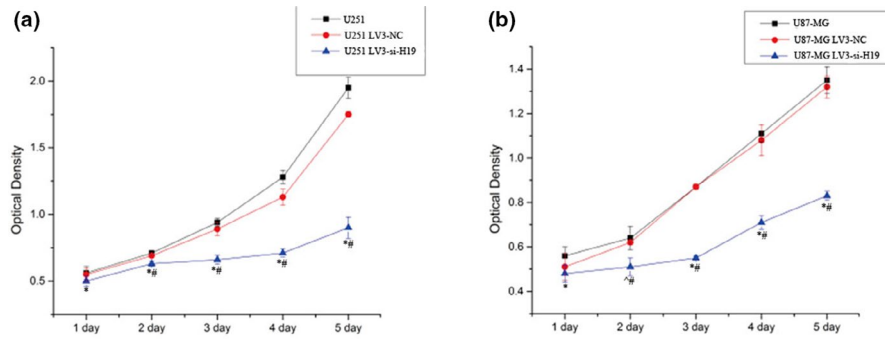


**FIGURE 2** Effects of *lncRNA-H19* knockdown on proliferation U251 and U87-MG cells. Growth curves of U251 cell (a) and U87-MG cell (b) with three treatments (untransfected control, LV3-NC transfected group, and LV3-si-H19-transfected group) determined by CCK-8 assay.  $^{\wedge}p < 0.05$ , versus untransfected group;  $^*p < 0.01$ , versus untransfected group;  $^{\#}p < 0.01$ , versus negative control group.

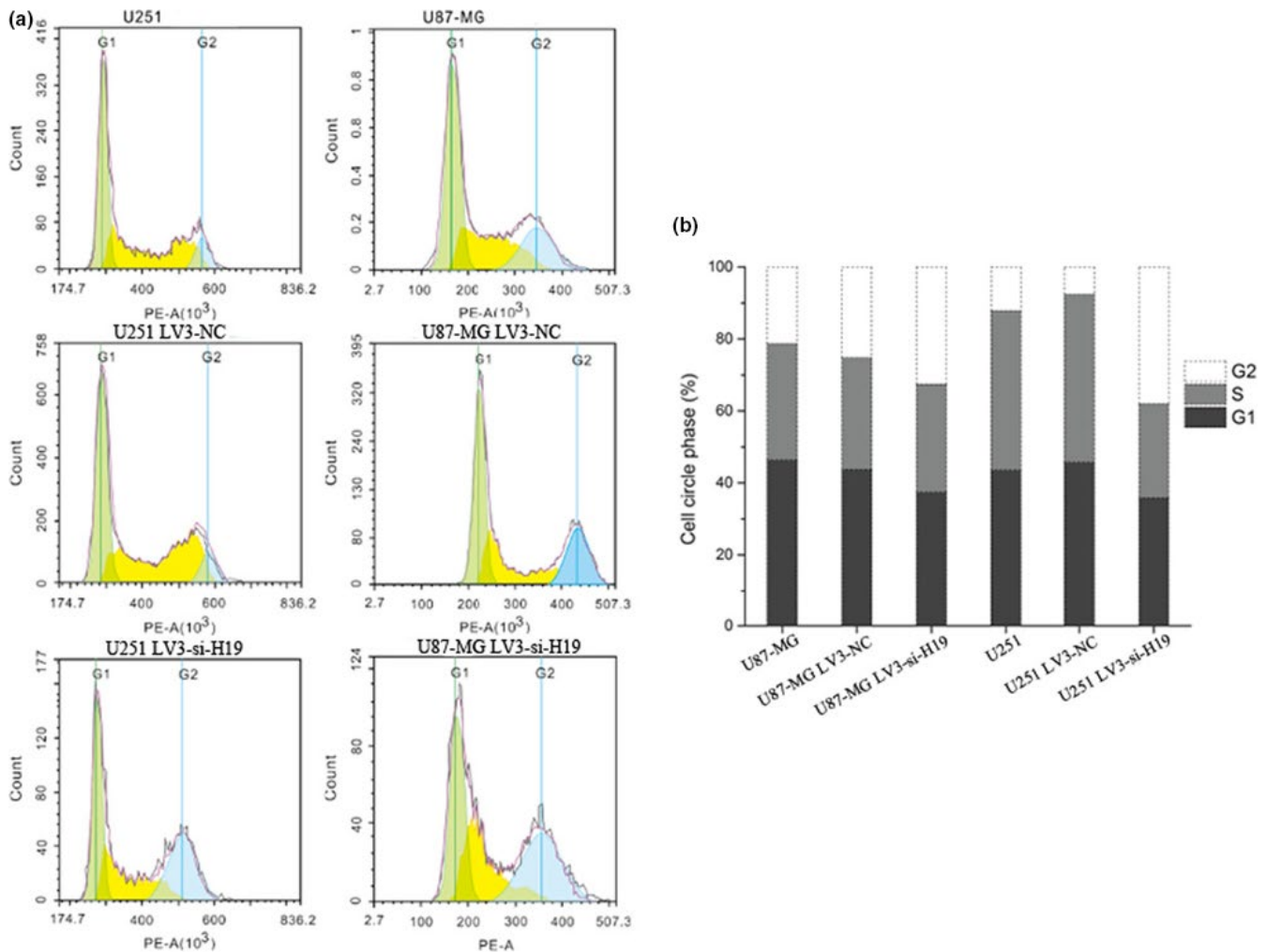


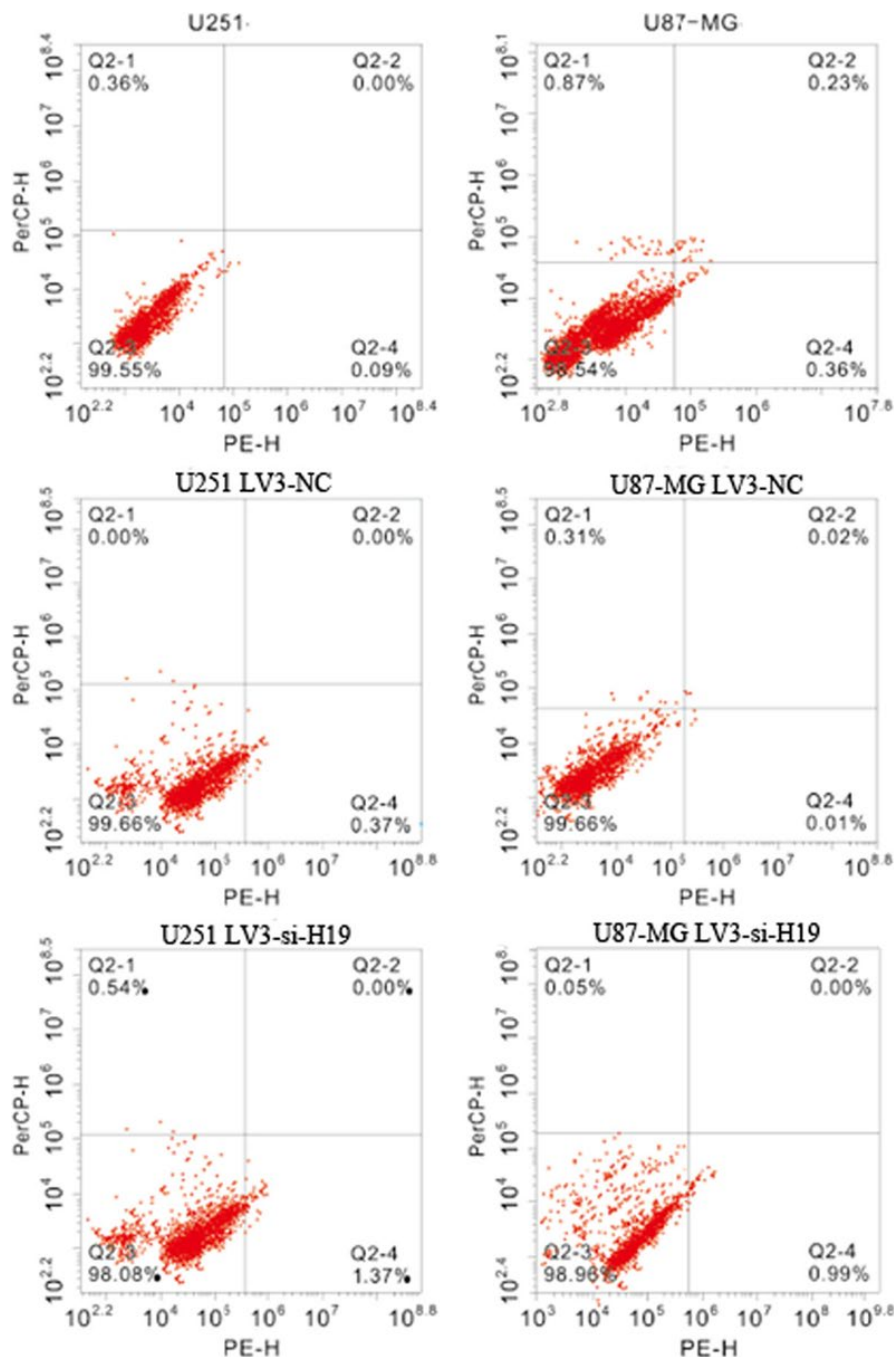
**FIGURE 3** Effect of *lncRNA-H19* knockdown on the cell cycle progression in the U251 and U87-MG cells. (a) The cells were analyzed by flow cytometry. (b) The statistic analysis of *lncRNA-H19* knockdown effect on the cell cycle progression.

### 3.6 | Tumor sphere formation assay

Formed spheres were counted for all visions. Furthermore, U251 / U87-MG cells formed standard sphere (marked as

$N_{C1}$ ), the remaining data (labeled  $N_{Nx}$ ) compared with  $N_{C1}$ . The effect of *lncRNA-H19* knockdown on sphere formation ability of U251 and U87-MG cells was analyzed using the following formula: inhibition rate =  $(N_{C1} - N_{Nx}) / N_{C1} \times 100\%$ .

**FIGURE 4** Detection of cell apoptotic rate by flow cytometry. No effect was observed on the apoptosis rate between LV3-si-H19-transfected group and LV3-NC group as well as untransfected group.



The amount of sphere formation was significantly reduced in LV3-si-H19-transfected group, compared with the LV3-NC group and untransfected group (Figure 6a), and inhibition rate of LV3-si-H19-transfected group was up to 57.5% (U251) and 47.5% (U87-MG), respectively (Figure 6b).

### 3.7 | Tumor growth in vivo

In the current study, the rats were used to estimate the effects of H19 expression on glioma progression in vivo. Tumor growth in each group is displayed in Figure 7a. Compared to controls, tumor growth in LV-si H19 group was obviously

slow. In control group, tumor was observed at 30 days after implantation, while tumor in LV-si H19 group could be obviously detected at 45 days after cell injection. Sixty days after injection, the average volume was  $8.70 \pm 0.25 \text{ mm}^3$  in U251 injected group and  $9.10 \pm 0.19 \text{ mm}^3$  in U251 LV-NC group, when tumor volume was significantly lower in LV-si H19 group ( $2.25 \pm 0.12 \text{ mm}^3$ ,  $p < 0.01$  for both). Tumor volume between untransfected control and negative control groups had no significant differences ( $p > 0.05$ ; Figure 7b).

Sixty days after injection, the rats were killed to isolate tumor specimens and tumor weight was estimated. The average weight in LV-si H19 group was significantly smaller than that in control groups (LV-si H19 group:  $0.44 \pm 0.12 \text{ g}$ , U251

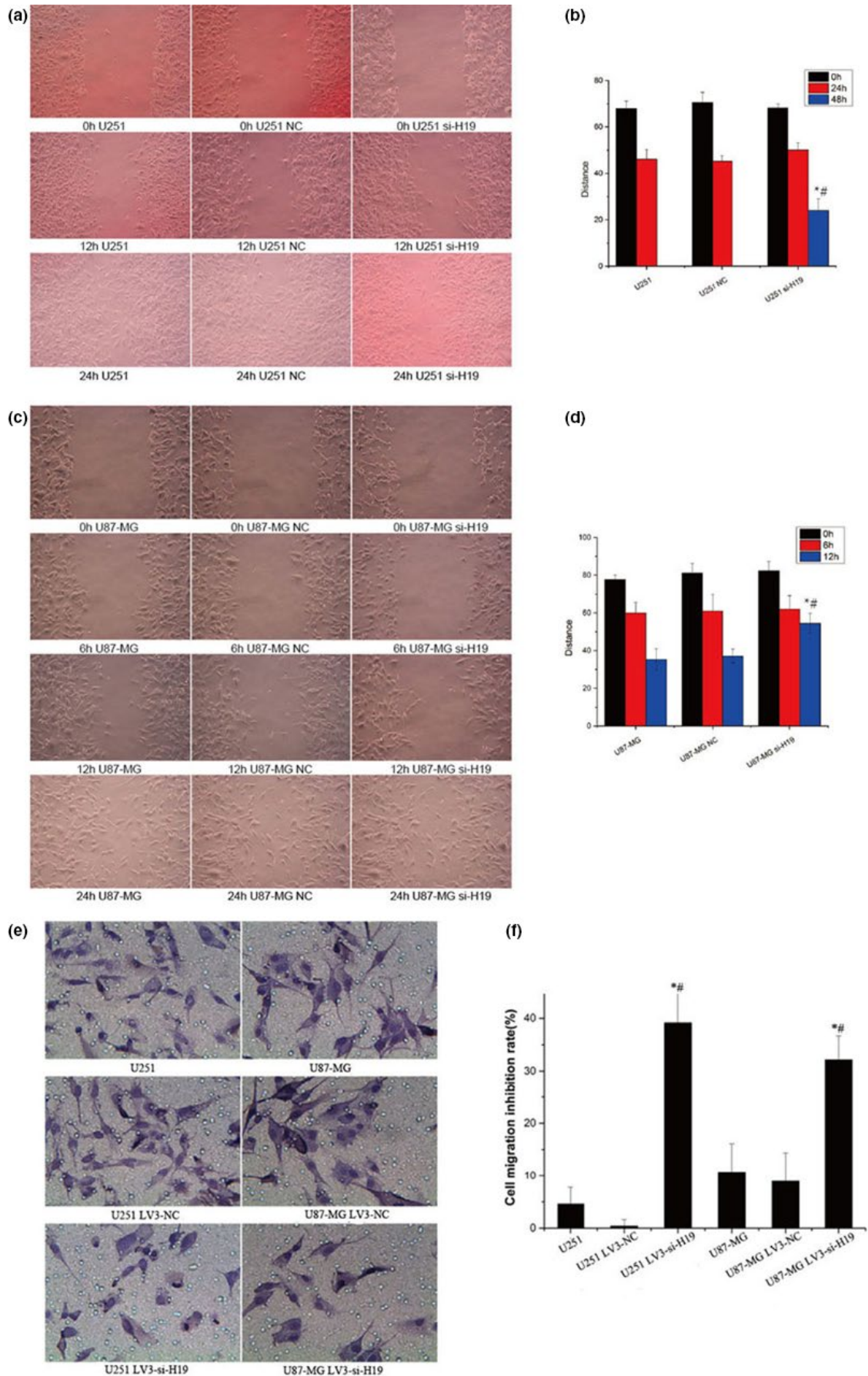


**FIGURE 5** Effect of *lncRNA-H19* knockdown on glioma cell's migration ability. (a–d) Wound healing assay was used to evaluate the migration of both U251 and U87-MG after silencing *lncRNA-H19*, ( $\times 100$ ). E–F. Transwell migration assay was used to evaluate the migration of both U251 and U87-MG after silencing *lncRNA-H19*.  $*p < 0.01$ , versus untransfected control group;  $\#p < 0.01$ , versus negative control group.

group:  $1.40 \pm 0.09$  g, LV-NC group:  $1.46 \pm 0.23$  g,  $p < 0.01$  for both). However, there was no difference between untransfected control and negative control groups ( $p = 0.687$ ; Figure 7c).

We also investigated the expression profiles of *H19* mRNA in each group. Compared to control groups, the expression levels of *H19* mRNA in U251 LV-si H19-transfected group were obviously decreased ( $p < 0.01$  for both). The untransfected control and negative control groups exerted no obvious differences in expression patterns of *H19* mRNA ( $p = 0.230$ ; Figure 7d).

In addition, the mean survival time of the rats was also compared between the study groups. The mean survival time was  $110.40 \pm 8.41$  days in rats injected with U251 LV-si H19 cells, and  $68.20 \pm 9.28$  days and  $69.40 \pm 11.30$  days in untransfected control and negative control groups, respectively. The survival time of LV-si H19 group was significantly longer than that of the control groups ( $p < 0.01$  for both). The untransfected control and negative groups showed similar survival time ( $p = 0.611$ ; Figure 7e).

## 4 | DISCUSSION

LncRNAs are involved in X chromosome silencing, chromatin modification, transcriptional regulation, small RNA processing, and other important regulatory processes (Rossi

& Antonangeli, 2014). It is confirmed that lncRNA plays an important regulatory role in a number of diseases especially tumors, and their dysregulated expression is observed in many human tumors (Gloss & Dinger, 2016). Moreover, previous studies have proven that *lncRNA-H19* could act as a tumor promoter or suppressor in different human cancers (Hua et al., 2016; Shi et al., 2014; Zhu et al., 2014; Zhuang et al., 2014). Colnot et al. (Yang et al., 2017) reported that the probability of *lncRNA-H19*-deficient mice suffering intestinal polyps was significantly higher than wild type in human colorectal cancer transplant mouse model. Ariel et al. (Hua et al., 2016) confirmed that the upregulation of *lncRNA-H19* was considered as an early sign of bladder cancer recurrence. Zhuang M et al. (Zhuang et al., 2014) found that *lncRNA-H19* expression was significantly increased in gastric carcinoma and cell lines. Upregulated *lncRNA-H19* could promote the proliferation of gastric cancer cells, but downregulated *lncRNA-H19* might enhance the apoptosis of gastric cancer cells. Shi Y et al. (Shi et al., 2014) studied biological function of *lncRNA-H19* expression in glioma and underlying mechanisms, and found that *lncRNA-H19* expression was related to glioma's grade. The expression of *lncRNA-H19* and its derivatives *miR-675* was higher in advanced grade glioma than low-grade ones.

In this study, we introduced si-H19 into glioma cells using lentiviral vector (Cambon et al., 2017; Fazio et al., 2017), and investigated biological function of *lncRNA-H19* in glioma.

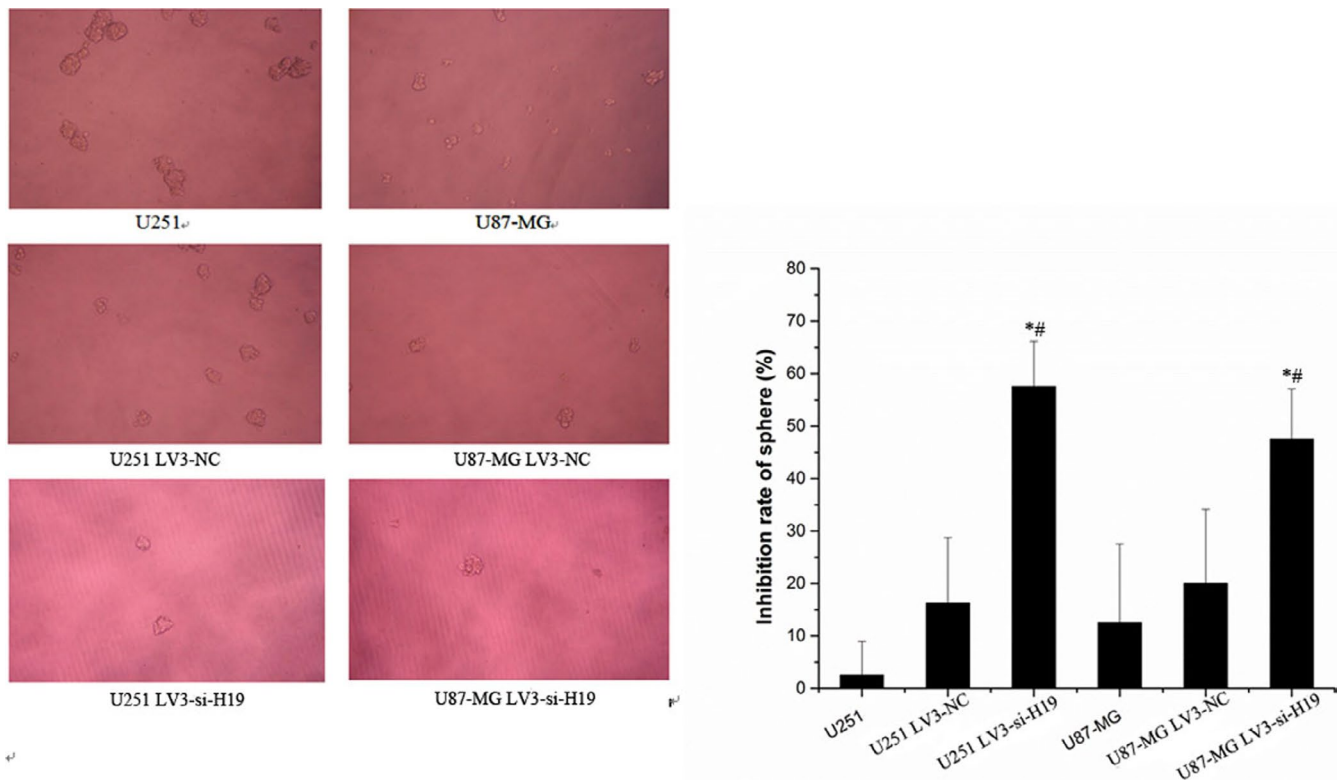
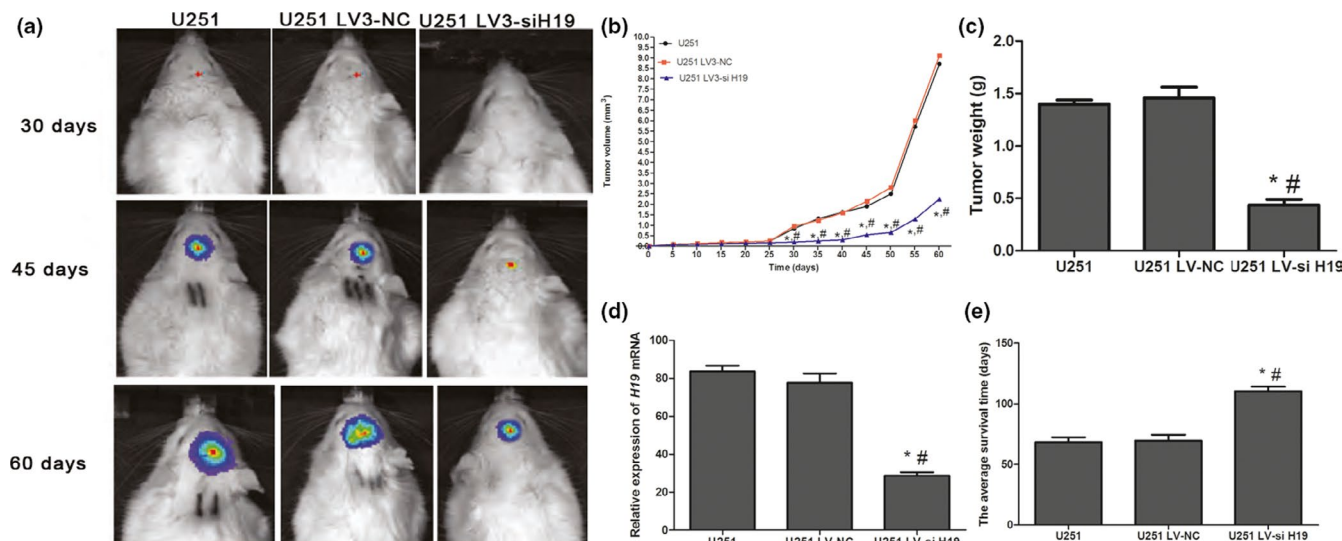


FIGURE 6 Tumor sphere formation result, ( $\times 100$ ). \* $p < 0.01$ , versus untransfected control group; # $p < 0.01$ , versus negative control group.



**FIGURE 7** Effects of *lncRNA-H19* knockdown on glioma growth and progression in vivo. (a) Bioluminescence imaging technique was performed to estimate tumor growth in rat models. (b) Tumor volume changes within 60 days after tumor implantation. The tumor volume in rats which were injected with U251 LV-si-H19 cells exhibited significantly small than that in the control groups. (c) Tumor weight estimation at 60 days after cell injection. Knockdown the expression of H19 could obviously reduce tumor weight in vivo. (d) The expression patterns of H19 in rats in each group. (e) The average survival time of rats in each group. Knockdown the expression of H19 could inhibit glioma growth and prolong the survival time of glioma animal models. \* $p < 0.01$ , versus untransfected control group; # $p < 0.01$ , versus negative control group.

Proliferation is a fundamental characteristic of tumor cells, so we tested the effect of *lncRNA-H19* on proliferation activity of glioma cells. After *lncRNA-H19* interference vector introduced into U251 and U87-MG cells, cell proliferation was detected via CCK8 assay, and the results showed that interfering *lncRNA-H19* gene inhibited the proliferation of U251 and U87-MG cells, which inversely proved that *lncRNA-H19* gene might promote tumor cell proliferation.

To determine the effect of *lncRNA-H19* on cell cycle distribution of U251 and U87-MG cells, we detected cell cycle using flow cytometry. Cell cycle distribution changed significantly after *lncRNA-H19* gene knockdown. Specifically, cell cycle progression was blocked, and a large number of cells were arrested in G2/M stage. This phenomenon also indicated that *lncRNA-H19* gene could promote the proliferation of U251 and U87-MG by pushing cell cycle progression smoothly. Apoptosis is one of the main types of programmed cell death, and many anticancer agents achieve therapeutic efficacy through inducing apoptosis (Dasari & Tchounwou, 2014; Hong et al., 2014; Safarzadeh, Sandoghchian Shotorbani, & Baradaran, 2014). To clarify the impact of *lncRNA-H19* gene on the apoptosis of glioma cells, the apoptosis of U251 and U87-MG cells was detected using flow cytometry. Interestingly, we did not observe significant difference in apoptosis after *lncRNA-H19* inhibition.

Cell migration is one of the basic features of tumor cells. Migratory ability of tumor cells can be determined via wound healing and transwell migration assay. Shi et al., (2014) found that interfering *lncRNA-H19* expression can suppress glioma cells' migration in 24 hr. In our study, we

extended corresponding incubation time for cells to further appraise their migrate ability. For wound healing assay, in U251 group, significant difference was observed at 48 hr instead of 24 hr between *lncRNA-H19* knockdown group and the negative control group; and in the U87-MG group, we found the cells in test group and control groups were all healed after 24 hr, which was different from previous results. In transwell migration assay, we carried out an experiment at 48 hr, and the difference was still significant. Results from the two experiments showed that *lncRNA-H19* hold the capability to regulate migration ability of glioma cells, which was in line with previous findings.

Sphere formation is one method for identifying self-renewal ability of tumor stem-like cells (Chao, Kan, Lu, & Chien, 2015). Iacopino et al., (2014) isolated tumor stem cells from three glioma cell lines L1, U87-MG, and U373 using ultralow-balling adhesion method. We also isolated tumor stem-like cells from U251 and U87-MG in our previous experiment. The present study suggested that *lncRNA-H19* could regulate the self-renewal of glioma cells, and this was the first time to report the involvement of *lncRNA-H19* in sphere-formation functions of U251 and U87-MG.

In addition, glioma animal models were constructed via injecting U251 cells in our study. Tumor volume and weight in U251 LV-si-H19 groups were significantly lowered compared to control groups. Moreover, survival time of these rats were obviously prolonged. The data revealed that knocking down *lncRNA-H19* expression could inhibit glioma growth and improve the survival of glioma.

The conclusion was in line with that from our in vitro experiments. *LncRNA-H19* might be a potential therapeutic target in treating glioma. However, there were still several limitations in the present study. First, clinical value of *lncRNA-H19* in glioma was not explored in our study. Due to the limited study period, the numbers of glioma cases in our study was not large enough to guarantee the significance of *lncRNA-H19* in clinic. Second, potential mechanisms underlying carcinogenic action of *lncRNA-H19* in glioma were not explored. Pull-down technique may be helpful to identify the target of *lncRNA-H19* in glioma, and proteomic analysis may provide more exact information on the mechanisms of *lncRNA H19* functioning in glioma. Further well-designed studies will be performed to address those mentioned issues.

In conclusion, *lncRNA-H19* plays a promoting role in glioma progression via enhancing cell proliferation, cell cycle, cell migrations, and sphere-forming function of glioma cell lines. *LncRNA-H19* may be a potential biomarker in the diagnosis and treatment of glioma in clinic.

## ACKNOWLEDGMENTS

None.

## CONFLICT OF INTEREST

The authors declare that they have no competing interests.

## AUTHOR CONTRIBUTION

P.L., X.H., and H.W. conceived and designed the experiments, analyzed the data, and wrote the paper. G.Y. and L.S. performed the experiments. All authors read and approved the final manuscript.

## DATA AVAILABILITY STATEMENT

All data generated or analyzed during this study are included in this article.

## ORCID

Liangfang Shen  <https://orcid.org/0000-0001-5509-8891>

## REFERENCES

- Allen, B. J., Huang, C. Y., & Clarke, R. A. (2014). Targeted alpha anti-cancer therapies: update and future prospects. *Biologics*, 8, 255–267. <https://doi.org/10.2147/BTT.S29947>
- Cambon, K., Zimmer, V., Martineau, S., Gaillard, M.-C., Jarrige, M., Bugi, A., ... Déglon, N. (2017). Preclinical evaluation of a lentiviral vector for huntingtin silencing. *Molecular Therapy - Methods & Clinical Development*, 5, 259–276. <https://doi.org/10.1016/j.omtm.2017.05.001>
- Chao, C. C., Kan, D., Lu, K. S., & Chien, C. L. (2015). The role of microRNA-30c in the self-renewal and differentiation of C6 glioma cells. *Stem Cell Research*, 14(2), 211–223. <https://doi.org/10.1016/j.scr.2015.01.008>
- Chen, L., Yao, H., Wang, K., & Liu, X. (2017). Long non-coding RNA MALAT1 regulates ZEB1 expression by sponging miR-143-3p and promotes hepatocellular carcinoma progression. *Journal of Cellular Biochemistry*, 118(12), 4836–4843. <https://doi.org/10.1002/jcb.26158>
- Dasari, S., & Tchounwou, P. B. (2014). Cisplatin in cancer therapy: molecular mechanisms of action. *European Journal of Pharmacology*, 740, 364–378. <https://doi.org/10.1016/j.ejphar.2014.07.025>
- Fazio, M., Avagyan, S., van Rooijen, E., Mannherz, W., Kaufman, C. K., Lobbardi, R., ... Zon, L. I. (2017). Efficient transduction of zebrafish melanoma cell lines and embryos using lentiviral vectors. *Zebrafish*, 14(4), 379–382. <https://doi.org/10.1089/zeb.2017.1434>
- Gloss, B. S., & Dinger, M. E. (2016). The specificity of long noncoding RNA expression. *Biochimica Et Biophysica Acta*, 1859(1), 16–22. <https://doi.org/10.1016/j.bbagr.2015.08.005>
- Gu, X., Wang, C. E., Wang, X., Ma, G., Li, Y., Cui, L., ... Li, K. (2015). Efficient inhibition of human glioma development by RNA interference-mediated silencing of PAK5. *International Journal of Biological Sciences*, 11(2), 230–237. <https://doi.org/10.7150/ijbs.9193>
- Hong, J. Y., Chung, H. J., Bae, S. Y., Trung, T. N., Bae, K., & Lee, S. K. (2014). Induction of cell cycle arrest and apoptosis by physcion, an anthraquinone isolated from rhubarb (Rhizomes of *Rheum tanguticum*), in MDA-MB-231 human breast cancer cells. *Journal of Cancer Prevention*, 19(4), 273–278. <https://doi.org/10.15430/JCP.2014.19.4.273>
- Hua, Q., Lv, X., Gu, X., Chen, Y., Chu, H., Du, M., & Zhang, Z. (2016). Genetic variants in lncRNA H19 are associated with the risk of bladder cancer in a Chinese population. *Mutagenesis*, 31(5), 531–538. <https://doi.org/10.1093/mutage/gew018>
- Iacopino, F., Angelucci, C., Piacentini, R., Biamonte, F., Mangiola, A., Maira, G., ... Sica, G. (2014). Isolation of cancer stem cells from three human glioblastoma cell lines: characterization of two selected clones. *PLoS One*, 9(8), e105166. <https://doi.org/10.1371/journal.pone.0105166>
- Li, J., Xue, W., Lv, J., Han, P., Liu, Y., & Cui, B. (2017). Identification of potential long non-coding RNA biomarkers associated with the progression of colon cancer. *Oncotarget*, 8(44), 75834–75843. <https://doi.org/10.18632/oncotarget.17924>
- Li, X.-F., Yin, X.-H., Cai, J.-W., Wang, M.-J., Zeng, Y.-Q., Li, M., ... Shen, M. (2017). Significant association between lncRNA H19 polymorphisms and cancer susceptibility: a meta-analysis. *Oncotarget*, 8(28), 45143–45153. <https://doi.org/10.18632/oncotarget.16658>
- Monnier, P., Martinet, C., Pontis, J., Stancheva, I., Ait-Si-Ali, S., & Dandolo, L. (2013). H19 lncRNA controls gene expression of the Imprinted Gene Network by recruiting MBD1. *Proceedings of the National Academy of Sciences of the United States of America*, 110(51), 20693–20698. <https://doi.org/10.1073/pnas.1310201110>
- Necsulea, A., Soumillon, M., Warnefors, M., Liechti, A., Daish, T., Zeller, U., ... Kaessmann, H. (2014). The evolution of lncRNA repertoires and expression patterns in tetrapods. *Nature*, 505(7485), 635–640. <https://doi.org/10.1038/nature12943>
- Prensner, J. R., Iyer, M. K., Sahu, A., Asangani, I. A., Cao, Q. I., Patel, L., ... Chinnaiyan, A. M. (2013). The long noncoding RNA SCHLAP1 promotes aggressive prostate cancer and antagonizes the SWI/SNF complex. *Nature Genetics*, 45(11), 1392–1398. <https://doi.org/10.1038/ng.2771>

- Rossi, M. N., & Antonangeli, F. (2014). LncRNAs: new players in apoptosis control. *International Journal of Cell Biology*, 2014, 473857. <https://doi.org/10.1155/2014/473857>
- Safarzadeh, E., Sandoghchian Shotorbani, S., & Baradaran, B. (2014). Herbal medicine as inducers of apoptosis in cancer treatment. *Advanced Pharmaceutical Bulletin*, 4(Suppl 1), 421–427. <https://doi.org/10.5681/apb.2014.062>
- Shi, Y., Wang, Y., Luan, W., Wang, P., Tao, T., Zhang, J., ... You, Y. (2014). Long non-coding RNA H19 promotes glioma cell invasion by deriving miR-675. *PLoS One*, 9(1), e86295. <https://doi.org/10.1371/journal.pone.0086295>
- Tracy, K. M., Tye, C. E., Page, N. A., Fritz, A. J., Stein, J. L., Lian, J. B., & Stein, G. S. (2018). Selective expression of long non-coding RNAs in a breast cancer cell progression model. *Journal of Cellular Physiology*, 233(2), 1291–1299. <https://doi.org/10.1002/jcp.25997>
- Wu, F., Zhang, C., Cai, J., Yang, F., Liang, T., Yan, X., ... Jiang, T. (2017). Upregulation of long noncoding RNA HOXA-AS3 promotes tumor progression and predicts poor prognosis in glioma. *Oncotarget*, 8(32), 53110–53123. <https://doi.org/10.18632/oncotarget.18162>
- Yang, W., Ning, N., & Jin, X. (2017). The lncRNA H19 Promotes Cell Proliferation By Competitively Binding to miR-200a and derepressing beta-catenin expression in colorectal cancer. *BioMed Research International*, 2017, 2767484. <https://doi.org/10.1155/2017/2767484>
- Zhang, Q., Su, M., Lu, G., & Wang, J. (2013). The complexity of bladder cancer: long noncoding RNAs are on the stage. *Molecular Cancer*, 12(1), 101. <https://doi.org/10.1186/1476-4598-12-101>
- Zhu, M., Chen, Q., Liu, X., Sun, Q., Zhao, X., Deng, R., ... Yu, J. (2014). lncRNA H19/miR-675 axis represses prostate cancer metastasis by targeting TGFBI. *FEBS Journal*, 281(16), 3766–3775. <https://doi.org/10.1111/febs.12902>
- Zhuang, M., Gao, W., Xu, J., Wang, P., & Shu, Y. (2014). The long non-coding RNA H19-derived miR-675 modulates human gastric cancer cell proliferation by targeting tumor suppressor RUNX1. *Biochemical and Biophysical Research Communications*, 448(3), 315–322. <https://doi.org/10.1016/j.bbrc.2013.12.126>

**How to cite this article:** Liu P, Huang X, Wu H, Yin G, Shen L. *LncRNA-H19* gene plays a significant role in regulating glioma cell function. *Mol Genet Genomic Med*. 2021;9:e1480. <https://doi.org/10.1002/mgg3.1480>